



Article

# Spatio-Temporal Variations in Soil Organic Carbon Stocks in Different Erosion Zones of Cultivated Land in Northeast China Under Future Climate Change Conditions

Shuai Wang 1, Xinyu Zhang 1, Qianlai Zhuang 2, Zijiao Yang 1, Zicheng Wang 1, Chen Li 3 and Xinxin Jin 1,\*

- <sup>1</sup> College of Land and Environment, Shenyang Agricultural University, Shenyang 110866, China; shuaiwang666@syau.edu.cn (S.W.); 2024240620@stu.syau.edu.cn (X.Z.); 2017500046@syau.edu.cn (Z.Y.); 2025200175@stu.syau.edu.cn (Z.W.)
- Department of Earth, Atmospheric, and Planetary Sciences, Purdue University, West Lafayette, IN 47907, USA; qzhuang@purdue.edu
- 3 Zhangwu County Agricultural Development Service Center, Fuxin 123200, China; chenli9527202410@163.com
- \* Correspondence: jinxinxin0218@syau.edu.cn; Tel.: +86-24-8848-7155

### Abstract

Soil organic carbon (SOC) plays a critical role in the global carbon cycle and serves as a sensitive indicator of climate change impacts, with its dynamics significantly influencing regional ecological security and sustainable development. This study focuses on the Songnen Plain in Northeast China—a key black soil agricultural region increasingly affected by water erosion, primarily through surface runoff and rill formation on gently sloping cultivated land. We aim to investigate the spatiotemporal dynamics of SOC stocks across different cultivated land erosion zones under projected future climate change scenarios. To quantify current and future SOC stocks, we applied a boosted regression tree (BRT) model based on 130 topsoil samples (0-30 cm) and eight environmental variables representing topographic and climatic conditions. The model demonstrated strong predictive performance through 10-fold cross-validation, yielding high R2 and Lin's concordance correlation coefficient (LCCC) values, as well as low mean absolute error (MAE) and root mean square error (RMSE). Key drivers of SOC stock spatial variation were identified as mean annual temperature, elevation, and slope aspect. Using a space-for-time substitution approach, we projected SOC stocks under the SSP245 and SSP585 climate scenarios for the 2050s and 2090s. Results indicate a decline of 177.66 Tg C (SSP245) and 186.44 Tg C (SSP585) by the 2050s relative to 2023 levels. By the 2090s, SOC losses under SSP245 and SSP585 are projected to reach 2.84% and 1.41%, respectively, highlighting divergent carbon dynamics under varying emission pathways. Spatially, SOC stocks were predominantly located in areas of slight (67%) and light (22%) water erosion, underscoring the linkage between erosion intensity and carbon distribution. This study underscores the importance of incorporating both climate and anthropogenic influences in SOC assessments. The resulting high-resolution SOC distribution map provides a scientific basis for targeted ecological restoration, black soil conservation, and sustainable land management in the Songnen Plain, thereby supporting regional climate resilience and China's "dual carbon" goals. These insights also contribute to global efforts in enhancing soil carbon sequestration and achieving carbon neutrality goals.

Academic Editor: Yu Liu

Received: 22 September 2025 Revised: 17 October 2025 Accepted: 21 October 2025 Published: 22 October 2025

Citation: Wang, S.; Zhang, X.; Zhuang, Q.; Yang, Z.; Wang, Z.; Li, C.; Jin, X. Spatio-Temporal Variations in Soil Organic Carbon Stocks in Different Erosion Zones of Cultivated Land in Northeast China Under Future Climate Change Conditions. *Agronomy* **2025**, *15*, 2459. https://doi.org/10.3390/agronomy15112459

Copyright: © 2025 by the authors. Licensee MDPI, Basel, Switzerland. This article is an open access article distributed under the terms and conditions of the Creative Commons Attribution (CC BY) license (https://creativecommons.org/licenses/by/4.0/).

Agronomy **2025**, 15, 2459 2 of 20

**Keywords:** soil organic carbon stocks; water erosion; geospatial machine learning; climate change scenarios.

### 1. Introduction

Soil organic carbon (SOC) is vital to global carbon cycles and ecosystem services, particularly in agricultural systems where it underpins soil health, fertility, and sustainable productivity [1,2]. In erosion-prone regions, SOC dynamics are complex due to interactions between soil degradation and carbon fluxes [3–5]. In northeast China's Songnen Plain, water-driven erosion redistributes soil carbon and reduces its stability and storage capacity [6,7]. Accurate assessment of SOC change in these areas is crucial for regional carbon accounting and climate adaptation planning [8–10]. However, existing studies often lack spatial detail and future projections, with limited integration of climate scenarios into SOC modeling [11,12]. Additionally, many treat erosion zones as uniform, overlooking important differences among slight, moderate, and severe erosion levels, each of which may respond differently to climatic changes [13–15]. This limits the effectiveness of land management and erosion control strategies.

Digital soil mapping (DSM) overcomes these limitations by enabling a high-resolution, spatially explicit estimation of SOC dynamics through the integration of field observations, remote sensing data, and environmental covariates [11,16,17]. Among machine learning approaches [18,19], the boosted regression tree (BRT) model has proven particularly effective, as it iteratively combines multiple regression trees using gradient boosting to capture complex nonlinear relationships and interactions among variables while preserving model generalizability [19]. BRT outperforms many conventional models in handling multi-source datasets, resisting outliers, and delivering interpretable results via measures of variable importance and partial dependence plots—making it especially well-suited for SOC prediction in conditions of limited sample availability and high spatial heterogeneity [12,18].

This study employs a BRT model combined with a space-for-time substitution method, enabling the projection of current soil–environment relationships into future climate scenarios. Unlike conventional methods, this framework allows for the assessment of spatio-temporal dynamics under distinct shared socioeconomic pathways (SSPs)—specifically SSP245 and SSP585—offering a robust basis for predicting SOC responses to midand late-century climate change [11,14,20,21]. By integrating erosion zone delineations, the model enhances fine-scale evaluation of SOC vulnerability and resilience across varying degrees of soil degradation.

The Songnen Plain represents an ideal study area due to its dual role as a vital grain-producing region and a hotspot for soil degradation [6,7]. Long-term intensive agriculture has substantially depleted SOC stocks and intensified erosion pressures in its black soil ecosystems, creating clearly defined erosion gradients that provide a natural experimental setting for analyzing SOC responses to geomorphic and climatic drivers [22,23]. The region's pronounced seasonal rainfall and freeze—thaw cycles further heighten its sensitivity to climate change, making it a critical case for assessing how future temperature and precipitation shifts may influence soil carbon loss [6,24]. Insights gained here are thus broadly applicable to temperate agricultural regions facing similar challenges and directly support China's dual carbon goals [25].

The primary innovation of this study lies in its integrated spatiotemporal assessment of SOC dynamics across cultivated lands under varying erosion intensities and future climate scenarios—a dimension largely absent from previous research, which has predominantly focused on static or non-erosion-specific SOC evaluations. This study aims to (1)

Agronomy **2025**, 15, 2459 3 of 20

quantify the spatial distribution of SOC stocks across cultivated lands in the Songnen Plain under varying erosion intensities; (2) project mid-century (2050s) and late-century (2090s) changes in SOC stocks under the SSP245 and SSP585 climate scenarios using a BRT-based modeling framework; (3) identify the dominant environmental drivers—including climate and topography—that regulate SOC dynamics within erosion zones; and (4) generate high-resolution spatial maps and provide evidence-based recommendations for soil conservation and climate-smart agricultural management. By integrating erosion zonation with future climate projections, this research intends to support regional carbon sequestration strategies and promote sustainable agriculture in northeastern China.

# 2. Materials and Methods

# 2.1. Overview of the Research Area

The study area is located on the Songnen Plain in Northeast China, formed by alluvial deposits from the Songhua and Nenjiang Rivers. As a key component of the Northeast Plain, it spans 43° N to 48° N and 122° E to 126° E (Figure 1). The region experiences a temperate continental monsoon climate, with a mean annual temperature of 3-5 °C and annual precipitation ranging from 400 to 600 mm, predominantly during summer. The concurrent rainy and warm seasons create favorable conditions for agricultural production. The plain underlies a fault basin developed since the Mesozoic Era, overlain by thick Quaternary unconsolidated sediments, primarily black calcareous soils and meadow soils. Notably, the black soil layer reaches depths of 30–100 cm, exhibiting high organic matter content and ranking among the most fertile soils in China [7]. This area constitutes one of the world's three major black soil regions. The topography is characterized by flat, open alluvial plains, sloping gently from west to east, with elevations between 120 and 300 m. A dense river network, along with numerous lakes and swamps, supports a distinctive grassland and wetland ecosystem rich in biodiversity and serving as a critical migratory corridor for birds. While regional water resources are abundant overall, their spatiotemporal distribution is uneven. Agriculture is dominated by maize, soybean, and rice cultivation, establishing the region as a vital national commodity grain base [6]. However, prolonged intensive development has triggered ecological challenges, including black soil degradation and declining groundwater levels, necessitating science-based management strategies to ensure sustainable development.

Agronomy **2025**, 15, 2459 4 of 20

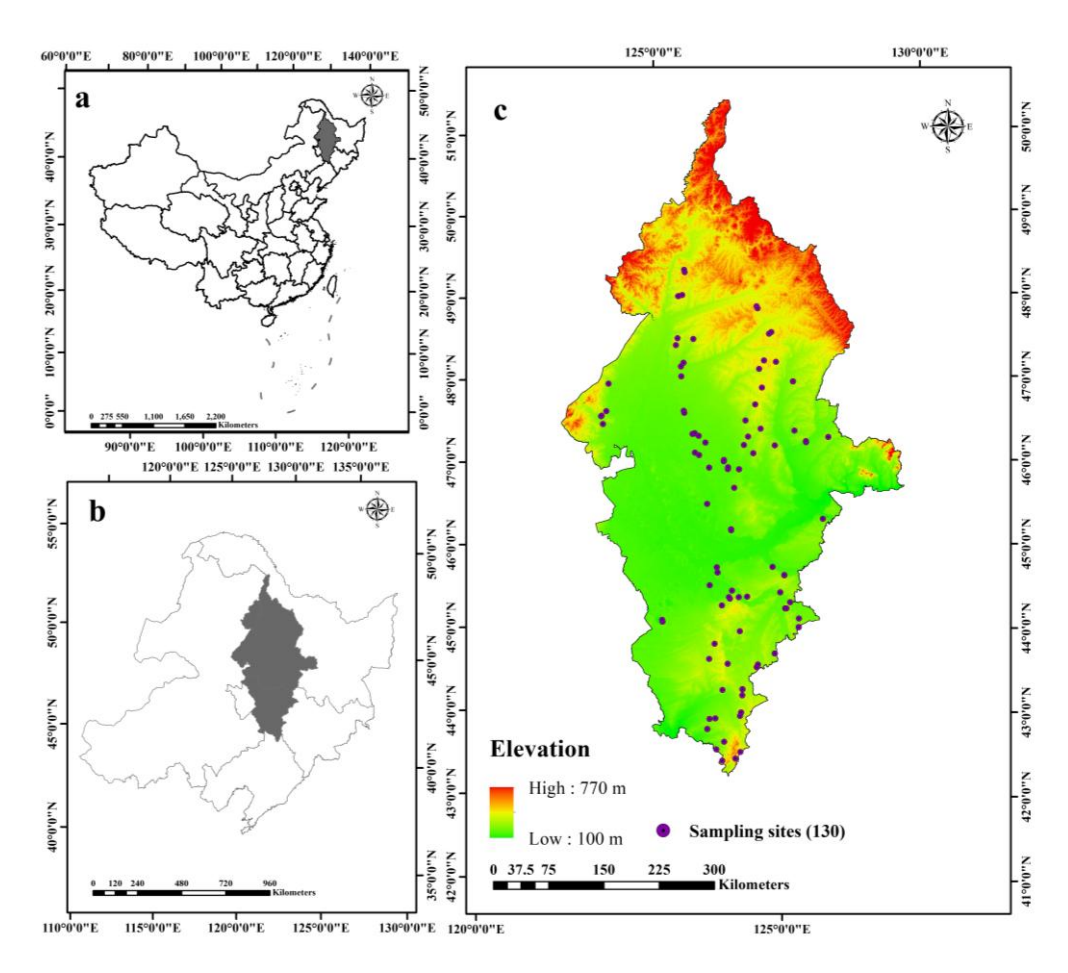


**Figure 1.** Location of the study area (**a**,**b**) and sampling point map (**c**) overlaid on the 90-m digital elevation model.

### 2.2. Collection of Soil Samples in the Field

Due to the extensive spatial extent of the Songnen Plain, traditional methods based on dense field sampling are inefficient and often fail to accurately capture the spatial distribution patterns of SOC stocks. To enhance resource efficiency and sampling effectiveness while ensuring robust spatial representation, this study adopted a purposive sampling strategy building upon the framework of Zhu et al. [26], incorporating key methodological improvements. The sampling design was developed through a four-stage process integrating environmental stratification, spatial variability analysis, and statistical power assessment. First, three primary environmental drivers of SOC variation—mean annual temperature (MAT), mean annual precipitation (MAP), and elevation—were selected and harmonized within a consistent 1-km spatial resolution geographic framework. Subsequently, the fuzzy c-means clustering algorithm was applied to these normalized environmental covariates, yielding 17 distinct landscape units that capture the major eco-geographical gradients across the study region.

The final sample size (n = 130) was determined through a comprehensive spatial variability analysis that integrated preliminary data with theoretical calculations. A pre-sampling spatial autocorrelation assessment, based on existing SOC data, revealed significant spatial clustering (Global Moran's I = 0.42, p < 0.01), justifying a stratified sampling design to effectively capture spatial heterogeneity. Applying the formula for stratified random sampling, the required sample size was derived from variance decomposition analysis, in which the total variance ( $\sigma^2$ \_total = 2.38) was partitioned into within-stratum ( $\sigma^2$ \_w = 1.72) and between-stratum ( $\sigma^2$ \_b = 0.66) components. To achieve a margin of error of ±0.5 g kg<sup>-1</sup> at a 95% confidence level, the minimum sample size was calculated as 118. This value was

Agronomy **2025**, 15, 2459 5 of 20

increased to 130 samples—approximately 7–8 per stratum—to accommodate potential field accessibility limitations and to enhance representation of transitional zones between landscape units.

The spatial distribution of sampling points was optimized through a weighted allocation strategy that accounted for both the area proportion and the variance in SOC within each stratum. Larger strata exhibiting higher internal variability were assigned a proportionally greater number of sampling points, while a minimum of five samples was retained in smaller strata to ensure sufficient spatial coverage. The sampling design was validated using semivariogram analysis of simulated configurations, confirming that the 130-point layout captured over 85% of the spatial variability in SOC distribution across the study region. All sample locations were accurately georeferenced with high-precision GPS devices (±3 m horizontal accuracy), and sampling depth was standardized at 0–30 cm in accordance with international soil carbon assessment protocols. This carefully designed framework ensures that the collected data adequately represent the spatial heterogeneity of SOC stocks while remaining operationally feasible under field conditions.

This study focuses on analyzing SOC stocks in cultivated soils within the 0-30 cm depth layer, based on well-established scientific and practical grounds. This soil layer is directly influenced by tillage practices and represents the most active zone for organic matter inputs—such as root exudates and crop residue return—and microbial activity. It is also highly responsive to short-term agricultural management interventions, including tillage systems and fertilization regimes, with changes in carbon storage closely linked to soil fertility and crop productivity. Furthermore, as an internationally standardized depth for soil monitoring, the 0-30 cm layer enables effective data harmonization and model calibration across studies. In contrast, while the 30–100 cm soil layer contains a substantial carbon pool, its carbon turnover occurs over centuries, primarily governed by mineral association and physical protection mechanisms, leading to delayed and uncertain responses to surface-level management. Additionally, deep soil sampling remains costly and methodologically inconsistent, and the absence of dedicated environmental covariates and mechanistic models for deep carbon dynamics undermines the reliability and scalability of large-scale assessments. Therefore, prioritizing the 0–30 cm layer allows for a more accurate and policy-relevant evaluation of the immediate effects of human activities and climate change, offering a practical foundation for developing agricultural carbon sequestration strategies.

At each site, approximately 1 kg of composite soil sample and a 100 cm³ undisturbed core were collected for laboratory analysis of SOC stocks and bulk density (BD), respectively. All samples were processed at the Laboratory Analysis and Testing Center of Shenyang Agricultural University under standardized protocols: SOC was measured via the dry combustion method using an Elementar Vario Max C/N analyzer (Germany), while BD was calculated after oven-drying the undisturbed cores at 105 °C for 48 h. This approach enhances both the spatial representativeness and coverage of sampling while maintaining high data quality.

### 2.3. Calculation of SOC Stocks

This study aims to simulate and predict the spatial differentiation characteristics of SOC stocks in the eroded cultivated ecosystem of the Songnen Plain in Northeast China under future climate change scenarios. For a soil profile comprising k soil layers, the SOC density of each layer can be calculated using the model developed by Batjes [27], which integrates key parameters such as SOC content, BD, and gravel content. This approach is well suited for spatially explicit simulations of multi-layer SOC stocks, thereby facilitating the understanding of the vertical distribution patterns and regional dynamic response

Agronomy **2025**, 15, 2459 6 of 20

mechanisms of agricultural SOC stocks in the context of climate change. The specific calculation formula was as follows [27]:

$$SOC \ stocks = \sum_{i=1}^{k} SOC \ content = \sum_{i=1}^{k} SOC \ concentration \times BD_{i} \times D_{i} \times (1 - S_{i})$$
 (1)

where SOC stocks (kg  $m^{-2}$ ) are calculated as the product of SOC concentration (g  $kg^{-1}$ ), bulk density (BD<sub>i</sub>, g cm<sup>-3</sup>), layer thickness (D<sub>i</sub>, m), and the complement of the volume fraction of soil fragments larger than 2 mm (S<sub>i</sub>), summed across each defined soil layer i. This formulation establishes a quantitative link between observable soil characteristics and the resulting SOC stocks per unit area, incorporating the contributions of both fine earth and coarse fragments within structured soil profiles.

### 2.4. Environmental Variables

This study selected 8 key terrain and climate environmental variables within the cultivated ecosystem of Northeast China to simulate and predict the spatial distribution patterns of SOC stocks under the SSP245 and SSP585 scenarios for the base year (2023) and future periods (2050s and 2090s). Considering that the selected environmental variables were derived from multiple heterogeneous data sources, spatial consistency and comparability were ensured by first resampling all variables to a uniform spatial resolution of 90 m using ArcGIS 10.2 (ESRI, Redlands, CA, USA), and subsequently projecting them into the Krasovsky\_1940\_Albers coordinate system to achieve spatial alignment. The preprocessed data were then imported into the R programming environment (R Development Core Team, 2013) [28] to develop a spatial prediction model for SOC, enabling accurate assessment and uncertainty analysis of regional SOC stock dynamics under various scenarios and time periods.

# 2.4.1. Topographic Variables

The Topographic variables used in this study were all derived from the Digital Elevation Model (DEM), which served as the foundation for digital terrain analysis and enabled the extraction of various terrain attribute parameters. The DEM data used in this study has a spatial resolution of 90 m and was obtained from the Geospatial Data Cloud platform of the Computer Network Information Center, Chinese Academy of Sciences (http://www.gscloud.cn). Based on this DEM, six key topographic variables were extracted: elevation, slope aspect (SA), slope gradient (SG), profile curvature (PC), topographic wetness index (TWI), and catchment area (CA). Among these, elevation, SA, SG, and PC were calculated using ArcGIS 10.2, while TWI and CA were derived using the System for Automated Geoscientific Analyses (SAGA) software (v. 2.1.4) [29]. Elevation refers to the vertical height of a location relative to a reference datum, and its spatial variation is typically associated with changes in hydrothermal conditions, vegetation types, and soil formation processes, which significantly influence the spatial distribution and dynamics of soil organic matter (SOM). As a major component of SOM, SOC stocks are highly responsive to climate change and human activities, and even minor variations in SOC can have significant implications for the global carbon cycle. SA affects the intensity of solar radiation and the angle of wind exposure, leading to notable differences in moisture and temperature conditions, light availability, and soil properties across different slope orientations. These variations contribute to the formation of localized microclimates, which in turn influence vegetation composition, biomass production, and litter input, ultimately resulting in spatial variability in SOC accumulation and decomposition processes. SG is a critical factor influencing soil erosion intensity, and its variation can indirectly affect the redistribution and stability of SOC by modifying erosion rates. TWI, which reflects the terrain's capacity to accumulate runoff, is commonly used to identify

Agronomy **2025**, 15, 2459 7 of 20

zones with high soil moisture or susceptibility to waterlogging. Higher TWI values generally indicate increased soil moisture, which may enhance the accumulation and preservation of organic matter. CA refers to the upstream drainage area contributing to a specific convergence point and is frequently used to estimate local surface runoff generation. It serves as a key topographic variable for predicting spatial patterns of SOC.

### 2.4.2. Climatic Variables

The climatic variables used in this study span the base year (2023) and two future periods (the 2050s and the 2090s). The climatic variables include gridded datasets of mean annual temperature (MAT) and mean annual precipitation (MAP), with a spatial resolution of 1 km. Historical MAT and MAP data for the reference period (2023) were obtained from the National Meteorological Information Center of the China Meteorological Administration (http://data.cma.cn/en, 30 August 2024). Based on daily precipitation and temperature observations from meteorological stations across Northeast China, spatial interpolation was conducted using the inverse distance weighting (IDW) method in ArcGIS 10.2 to generate continuous surfaces covering the entire study region. Future climate projections were derived from the WorldClim dataset (https://www.worldclim.org), representing average conditions for the periods 2041-2060 (2050s) and 2081-2100 (2090s), under two shared socioeconomic pathways: SSP245 and SSP585. These scenarios were selected to assess the response of SOC stocks under varying socioeconomic development trajectories and policy interventions, thereby providing a scientific basis for regional carbon management strategies. SSP245 represents a medium-low emission scenario, projecting a radiative forcing of approximately 4.5 W/m<sup>2</sup> by 2100, assuming moderate climate mitigation efforts. In contrast, SSP585 represents a high-emission scenario with a radiative forcing of 8.5 W/m<sup>2</sup>, reflecting a future of continued high greenhouse gas emissions under an energyintensive development model. This scenario enables the evaluation of SOC dynamics and its climate feedback potential in the absence of effective mitigation measures.

### 2.5. Prediction Models

In this study, a combination of the BRT model and space-for-time substitution method (STS) was used to simulate and predict the spatiotemporal dynamics of SOC stocks in the topsoil (0–30 cm) of different soil erosion areas in the Songnen Plain of Northeast China during historical periods and future scenarios. In addition, it should be emphasized that this study focuses on the spatiotemporal dynamics of SOC stocks in cultivated soils across different erosion zones of the Songnen Plain, China. Consequently, sampling was restricted to cultivated land, and predictive simulations were not performed for other land use types such as forestland, grassland, or wetlands. As a result, areas corresponding to non-cultivated land uses appear blank in the subsequent prediction maps, accurately reflecting the scope of this study. The specific technical roadmap was shown in Figure 2.

Agronomy **2025**, 15, 2459 8 of 20

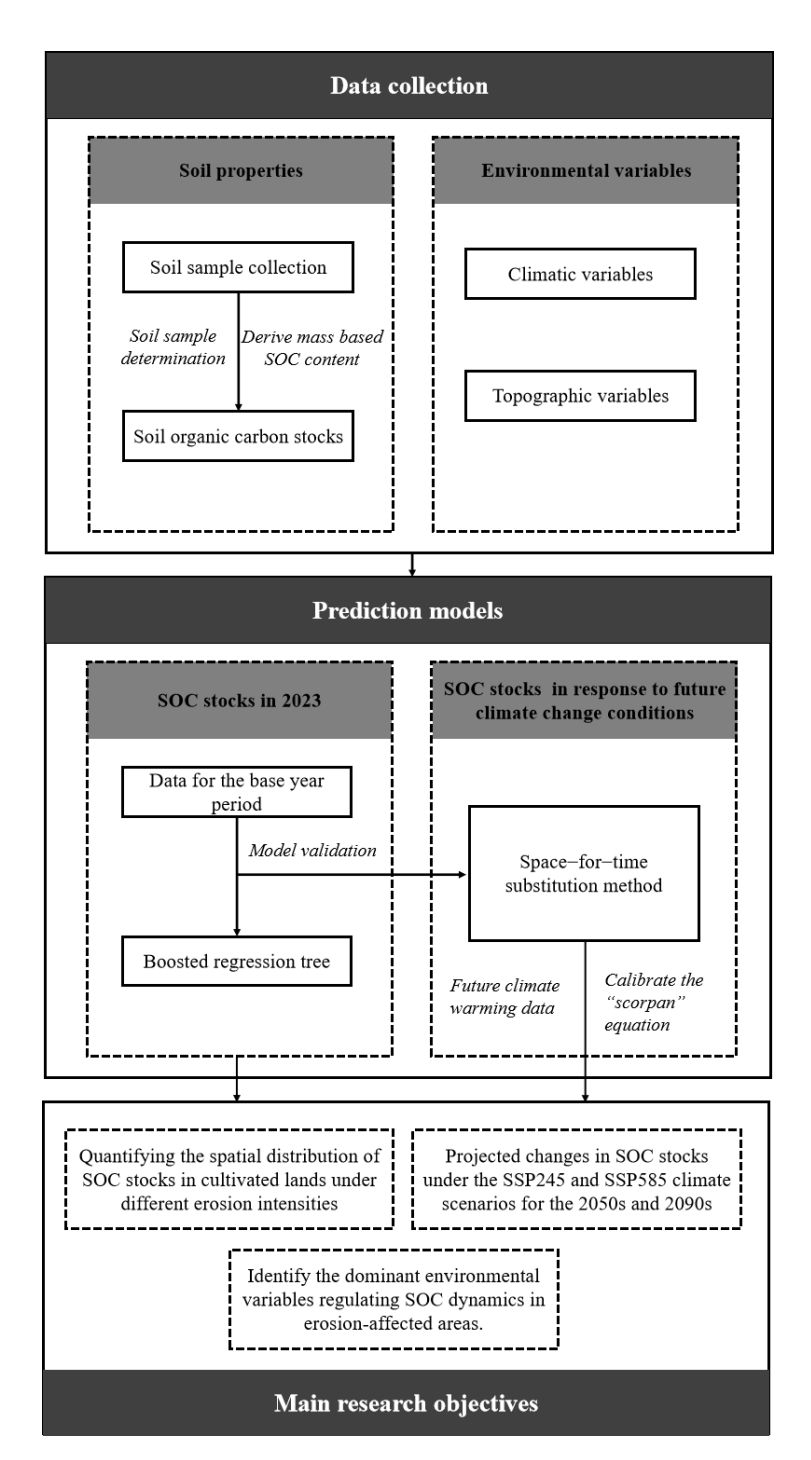


Figure 2. Schematic diagram of research technology roadmap.

# 2.5.1. Boosted Regression Trees

BRT is a machine learning algorithm proposed by Elith et al. [18] that effectively captures complex nonlinear relationships between dependent and independent variables. This model combines the characteristics of regression trees and boosting methods: regression trees handle variable relationships through recursive binary segmentation, while boosting methods combine multiple weak prediction models (usually shallow trees) in a progressive manner, gradually reducing prediction errors and forming strong predictors [12]. Unlike traditional minimalist models, BRT has a high degree of flexibility and can handle both continuous and categorical predictor variables simultaneously [19]. It is insensitive to missing values and does not require prior data conversion or outlier removal. In addition, the model can automatically identify the interaction effects between variables

Agronomy **2025**, 15, 2459 9 of 20

and is suitable for modeling data with complex ecological relationships [18]. In the actual fitting process, BRT optimizes key hyperparameters through cross validation, including learning rate (LR, controlling the contribution of each tree), tree complexity (TC, determining the branch depth and interaction complexity of the tree), bag fraction (BF, specifying the proportion of self-serving sub samples in each round), and number of trees (NT). This study used the "dismo" and "gbm" packages in the R language [28] to establish a model. After parameter tuning, the optimal configuration was determined to be LR = 0.025, TC = 8, BF = 0.75, NT = 2500. This combination significantly improves the prediction accuracy and robustness of the model in cross-validation, demonstrating better performance than traditional statistical methods.

# 2.5.2. Space-for-Time Substitution Method

The formation and evolution of soil are profoundly influenced by environmental factors, including climate, biological activity, topography, and parent material. The "scorpan" soil landscape model introduced by McBratney et al. [16] offers a theoretical framework for predicting spatiotemporal variations in soil properties, such as SOC stocks. By calibrating this model and applying it to future climate projections and land use scenarios, SOC stocks can be projected for specific time periods using the space-for-time substitution (STS) method. STS has been widely applied in SOC dynamic modeling across countries such as the United States, Australia, and Brazil [11,14,20,21]. However, its application to future predictions remains challenging, primarily due to the absence of actual SOC measurements for validation, which limits the direct assessment of prediction uncertainty and accuracy [11]. This study focuses on eroded croplands in the Songnen Plain of Northeast China. First, based on environmental variables and field sampling data from 2023, we conducted a spatially explicit simulation of topsoil SOC stocks. Subsequently, assuming that topography and parent material remain relatively stable in the future (2050s and 2090s), the STS model was employed to isolate and analyze the spatiotemporal impacts of climate change and land use dynamics on SOC stocks, aiming to reveal the trajectory of SOC stock evolution under different SSPs.

### 2.6. Model Validation

The accuracy of predicting SOC stocks in future periods (2050s and 2090s) largely depends on the reliability of prediction models developed for the historical period using 2023 data. This reliance arises because the functional relationship between future SOC stocks and environmental variables is extrapolated from the current model. To systematically evaluate the performance of the BRT model in predicting SOC stocks in 2023, this study employed 10-fold cross-validation and assessed four evaluation metrics: Mean Absolute Error (MAE), Root Mean Square Error (RMSE), Coefficient of Determination (R²), and Lin's Concordance Correlation Coefficient (LCCC) [30]. These metrics provide a multi-dimensional assessment of model performance, encompassing prediction bias, error magnitude, explanatory power, and agreement between predicted and observed values. The calculation formulas are as follows:

$$MAE = \frac{1}{n} \sum_{i=1}^{n} |a_i - b_i|$$
 (2)

$$RMSE = \sqrt{\frac{1}{n} \sum_{i=1}^{n} (a_1 - b_1)^2}$$
 (3)

$$R^{2} = \frac{\sum_{i=1}^{n} \left( a_{i} - \bar{b_{i}} \right)^{2}}{\sum_{i=1}^{n} \left( b_{i} - \bar{b_{i}} \right)^{2}}$$
(4)

$$LCCC = \frac{2r\partial_a\partial_b}{\partial_a^2 + \partial_b^2 + \left(\bar{a} + \bar{b}\right)^2}$$
 (5)

During the model validation process, let  $a_i$  and  $b_i$  denote the observed and predicted values of the i-th sample, respectively, while a and b, represent the arithmetic means of the observed and predicted values. Let a and a denote the variances of the corresponding data series, n be the total sample size, and r be the Pearson correlation coefficient between the predicted and observed values.

### 3. Results

### 3.1. Descriptive Statistics

The descriptive statistical results of SOC stocks and related environmental variables in 130 topsoil samples collected in 2023 were summarized in Figure 3. Analysis showed that the variation range of SOC stocks was  $1.32-17.46 \text{ kg m}^{-2}$ , with an average value of  $6.30 \text{ kg m}^{-2}$ . Its skewness and kurtosis coefficients were 1.16 and 1.70, respectively, indicating that the variable deviated from normal distribution. Therefore, this study performed a logarithmic transformation on the SOC stock data to meet the statistical requirements of subsequent modeling. To further evaluate the correlation between the converted SOC stocks and environmental variables, we calculated the Pearson correlation coefficient (Table 1). The results showed that SOC stocks were significantly positively correlated with elevation (r = 0.42) and MAT (r = 0.42), while significantly negatively correlated with MAP (r = -0.62). There was a strong correlation between climatic variables, especially MAP, and SOC stocks, indicating that climatic variables played an important role in driving the spatial differentiation of SOC stocks in the Songnen Plain region of northeastern China.

**Table 1.** Pearson correlation analysis between soil organic carbon (SOC) stocks and environmental variables based on 130 sampling sites data.

Property	SOC Stocks	ELE	SG	SA	PC	CA	TWI	MAP
ELE	0.42 **							
SG	0.11	0.42 **						
SA	0.06	-0.08	-0.16					
PC	-0.10	0.01	-0.10	-0.20 *				
CA	0.09	-0.51 **	-0.49 **	0.21 *	-0.05			
TWI	-0.04	-0.62 **	-0.80 **	0.21 *	0.06	0.79 **		
MAP	-0.62 **	0.35 **	-0.02	-0.28 **	0.07	-0.18 *	-0.59 **	
MAT	0.42 **	-0.43 **	-0.16	-0.20 *	-0.05	0.79 **	-0.04	0.51 **

**Note:** ELE, elevation; SG, slope gradient; SA, slope aspect; PC, profile curvature; CA, catchment area; TWI, topographic wetness index; MAP, mean annual precipitation; MAT, mean annual temperature. \*, p < 0.01; \*\*, p < 0.05.

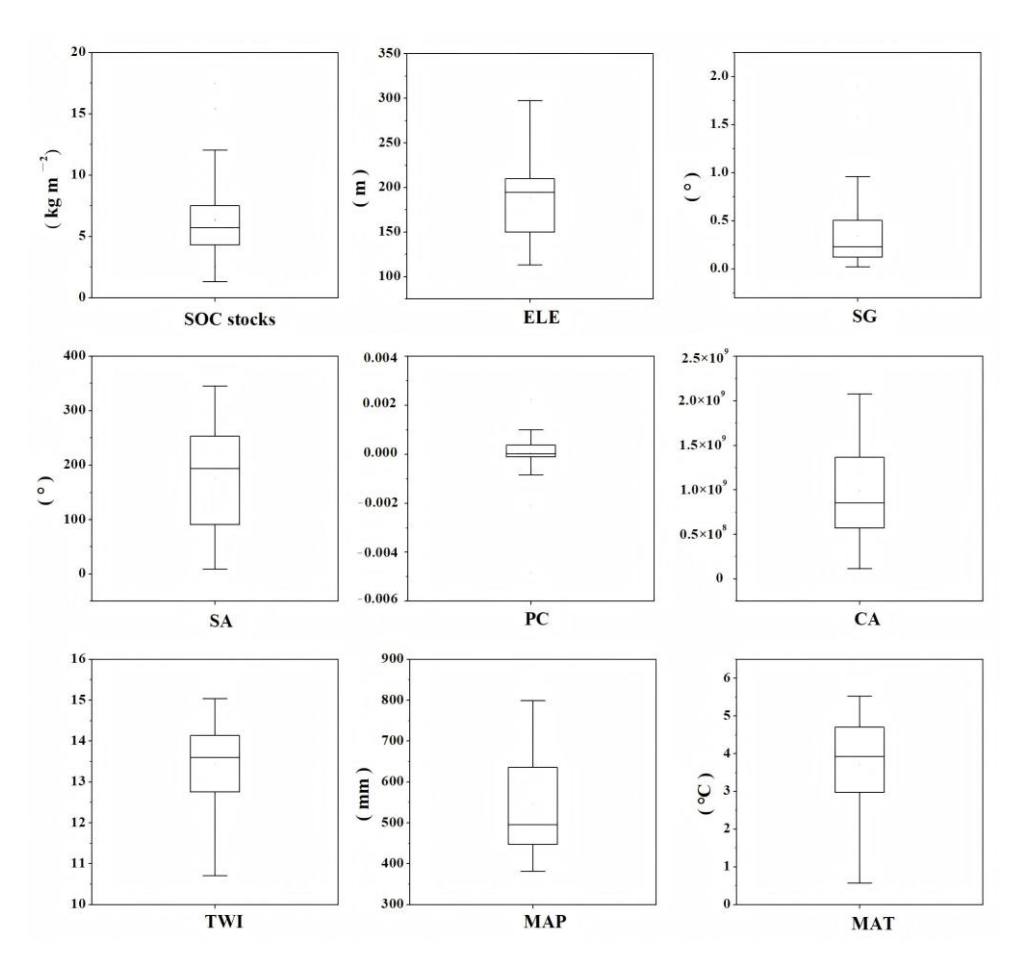


**Figure 3.** Boxplot of soil organic carbon (SOC) stocks and environmental variables at sampling sites. Note: ELE, elevation; SG, slope gradient; SA, slope aspect; PC, profile curvature; CA, catchment area; TWI, topographic wetness index; MAP, mean annual precipitation; MAT, mean annual temperature.

### 3.2. Model Performance and Uncertainty

Based on the 10-fold cross-validation method, a systematic evaluation was conducted to assess the performance of the BRT model in predicting the spatial distribution of topsoil SOC stocks. The validation results demonstrated that the BRT model achieves high predictive accuracy, with R<sup>2</sup> and LCCC of 0.52 and 0.65, respectively. The MAE and RMSE are 1.45 kg m<sup>-2</sup> and 2.03 kg m<sup>-2</sup>, respectively (Table 2). These statistical metrics indicated that the model effectively captures 52% of the spatial variability in SOC stocks across the study region in 2023, demonstrating its superior predictive capability (Table 2). To further evaluate model stability, we performed 100 iterations and calculated an average standard deviation of 0.41 ± 0.09 kg m<sup>-2</sup> (Figure 4). This low variation suggested that the BRT model exhibited low uncertainty and stronger robustness in predicting SOC stocks in the Songnen Plain region of northeastern China. Spatially, topsoil SOC stocks in those regions in 2023 display a clear northward-increasing gradient. High SOC stock values were predominantly found in the central and northern black soil regions and humid mountainous areas, likely due to greater organic matter inputs and more favorable soil moisture and thermal conditions. In contrast, lower SOC values were observed in southern areas characterized by intensive agricultural practices and relatively arid climates, highlighting the combined influence of anthropogenic activities and natural environmental factors on carbon sequestration.

Table 2. Summary statistics of soil organic carbon (SOC) stock prediction performance of boosted
regression tree (BRT) model in 2023.

Index	MAE	RESE	R <sup>2</sup>	LCCC
Min.	1.40	1.98	0.43	0.61
1stQu.	1.42	2.00	0.49	0.64
Median	1.43	2.01	0.52	0.66
Mean	1.45	2.03	0.52	0.65
3rdQu.	1.47	2.07	0.54	0.67
Max.	1.50	2.10	0.59	0.68

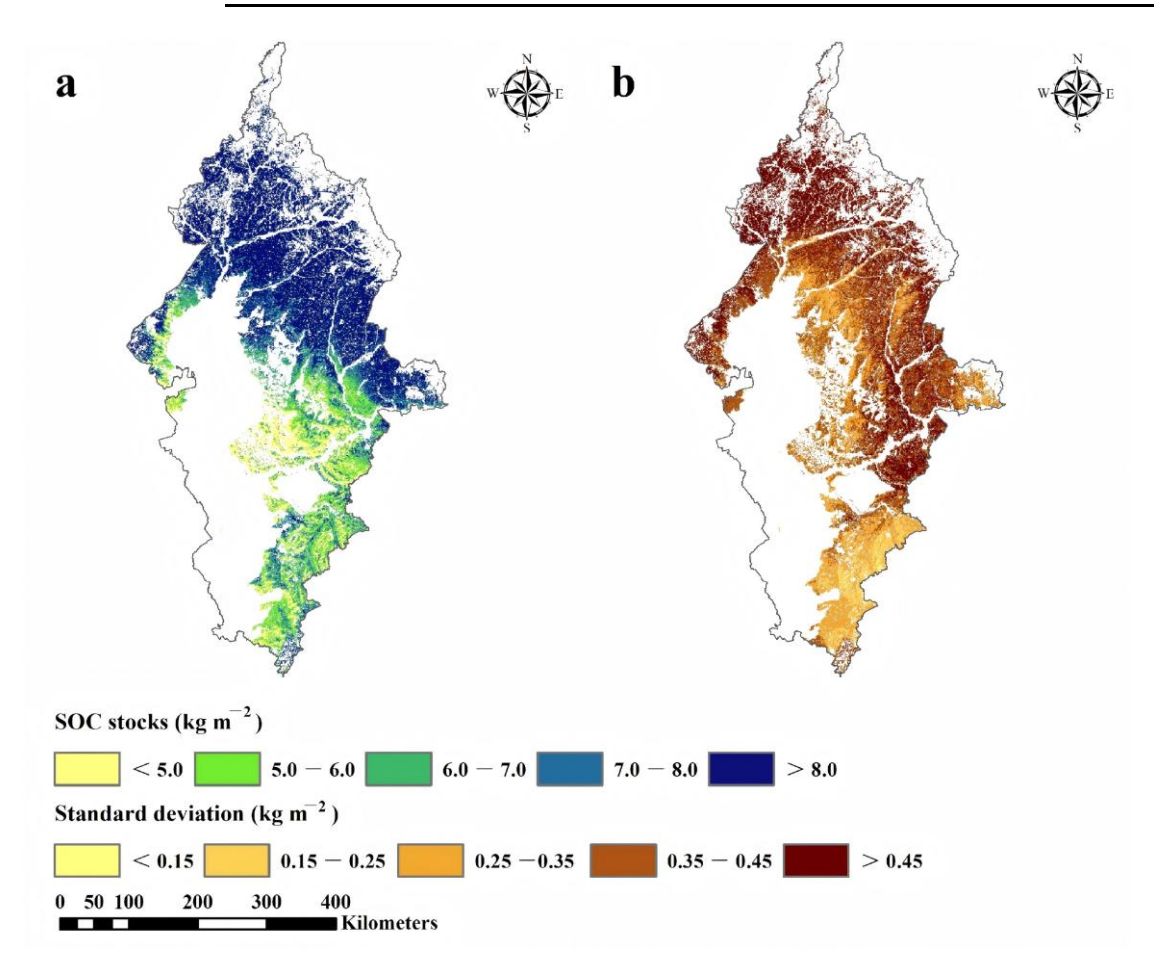


**Figure 4.** Spatial distribution (a) and Standard deviation (b) maps of average soil organic carbon density (SOCD) based on 100 iterations of the BRT model in 2023.

### 3.3. Relative Importance of Environmental Variables

After 100 iterations of the BRT model, the average relative importance (RI) of 8 environmental variables was computed, with RI values normalized to sum to 100% for comparative purposes. The results revealed a marked difference in the influence of topographic and climatic variables on the spatial distribution of SOC stocks: topographic variables accounted for 64% of the total RI, substantially exceeding that of climatic variables (36%) (Figure 5). Among all predictors, MAT, elevation, and SA emerged as the three most influential variables, collectively contributing 60% of the total RI. This indicated that thermal conditions, elevation, and surface morphology were the primary drivers of spatial heterogeneity in SOC within the study region. Further analysis suggested that MAT regulated microbial metabolic activity and the decomposition of organic matter, thereby influencing carbon accumulation; elevation acts as an integrative proxy for the redistribution of water and heat, indirectly shaping vegetation patterns and primary productivity;

SG, in turn, governed the redistribution and stability of organic carbon by modulating surface material transport, hydrological processes, and erosion-deposition dynamics. These findings enhance our understanding of the mechanisms underlying the spatial differentiation of SOC under multi-factor interactions.

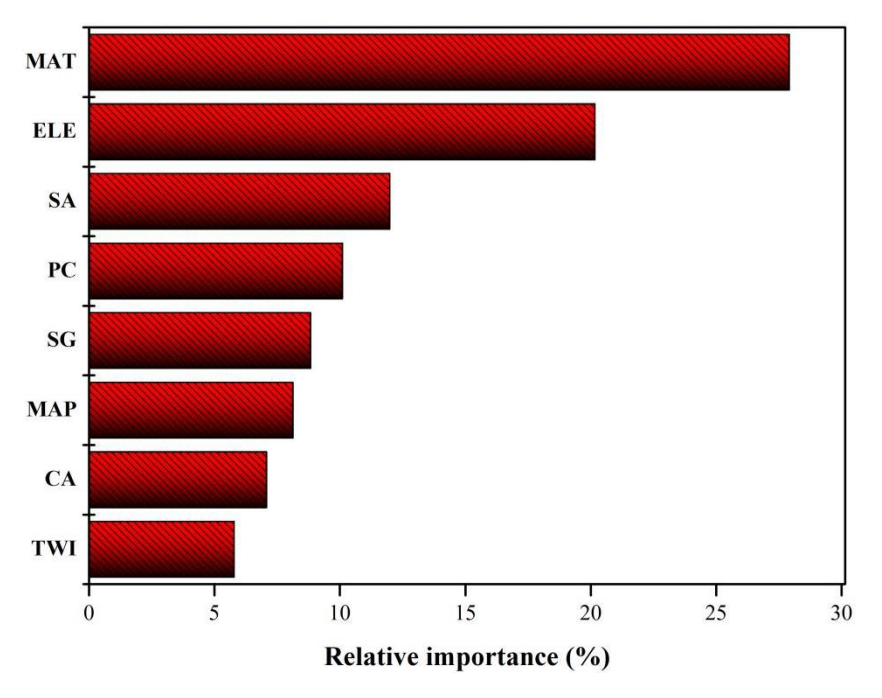


**Figure 5.** Relative importance (RI) of different environmental variables based on 100 iterations of the BRT model in 2023. SG, slope gradient; SA, slope aspect; PC, profile curvature; CA, catchment area; TWI, topographic wetness index; MAP, mean annual precipitation; MAT, mean annual temperature.

# 3.4. Spatial Distribution Variation in SOC Stocks Under Various Erosion Types

Based on a modeling framework integrating the BRT model and STS, this study simulated the spatial distribution of SOC stocks in the topsoil across different soil erosion zones in the Songnen Plain of Northeast China in 2023, and projected its changing trends under multiple climate scenarios. The results indicate that the coupled BRT-STS model performs well in predicting SOC stocks for the 2050s and 2090s. In 2023, SOC stocks were predominantly located in areas experiencing slight and light and water erosion, amounting to 496.18 Tg C and 159.88Tg C, respectively, accounting for 68% and 22% of the total SOC stocks (Table 3). Under future climate scenarios, SOC stocks are projected to undergo significant declines: by the 2050s, reductions of 177.66 Tg C and 186.44 Tg C were expected under the SSP245 and SSP585 scenarios, respectively, relative to the 2023 baseline; by the 2090s, further decreases were projected compared to the 2050s, with additional losses of 2.84% and 1.41% under the respective scenarios. Spatially, the distribution patterns of SOC stocks in the 2050s and 2090s remain relatively consistent under both SSP245 and SSP585 (Figure 6). High-value areas were primarily concentrated in the northern regions characterized by complex terrain and high vegetation cover, whereas low values prevail in the southern regions influenced by intensive human activities and a relatively arid climate. This spatial pattern underscores the combined regulatory effects of natural factors (e.g., climate, topography) and anthropogenic activities on SOC distribution, and suggests that, despite varying emission pathways, the regional natural environmental background remains the dominant control on SOC spatial heterogeneity. These findings hold important scientific implications for understanding the response mechanisms of soil carbon pools under concurrent climate change and human disturbance.

Agronomy **2025**, 15, 2459 14 of 20

Table 3. Summary statistics of soil organic carbon (SOC) stocks under various erosion types across
different climate scenarios and time periods.

Exector Type	Level	Area (km²)	2023 (Tg)	2050s (Tg)		2090s (Tg)	
Erosion Type				SSP245	SSP585	SSP245	SSP585
	Slight	62,660.00	496.18	389.09	381.92	377.12	376.77
Water erosion	Light	18,618.00	159.88	116.24	115.05	113.23	112.99
water erosion	Moderate	7665.00	74.75	48.27	47.84	47.49	47.36
	Severe	155.00	1.24	0.82	0.83	0.83	0.83
	Slight	21.00	0.13	0.11	0.11	0.11	0.11
Wind erosion	Light	5.00	0.03	0.03	0.03	0.03	0.03
wind erosion	Moderate	7.00	0.04	0.04	0.04	0.04	0.04
	Severe	2.00	0.02	0.01	0.01	0.01	0.01
Total		89,133.00	732.27	554.61	545.83	538.86	538.14

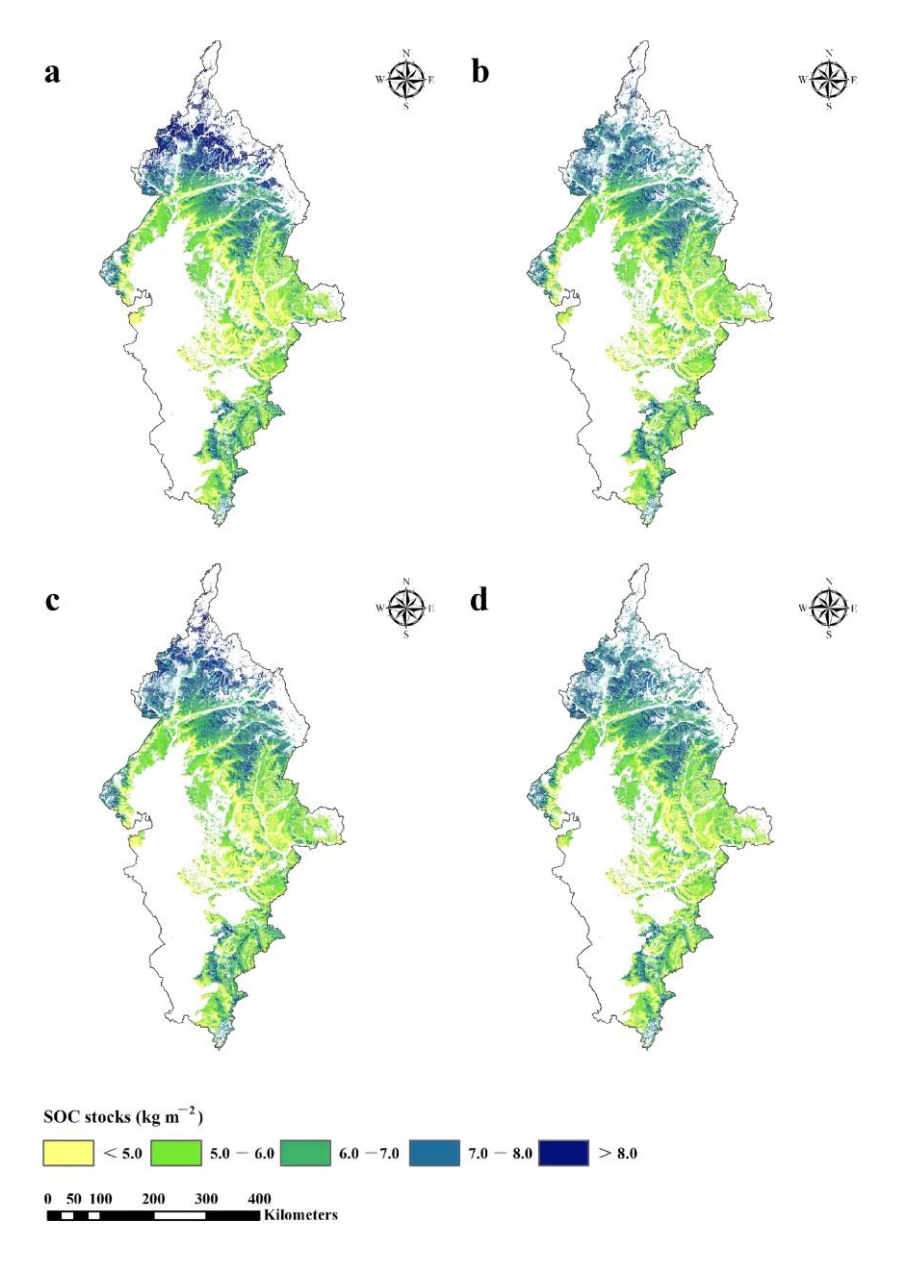


**Figure 6.** Spatial distribution map of soil organic carbon (SOC) stocks under SSP245 ((a) for the 2050s, (b) for the 2090s) and SSP585 ((c) for the 2050s, (d) for the 2090s) scenarios based on a boosted regression tree (BRT) model and the space-for-time substitution (STS) method.

### 4. Discussion

### 4.1. Controls of SOC Stocks

This study utilized terrain and climate variables as core predictive variables to conduct historical retrospective analyses and future scenario simulations of topsoil SOC stocks in different soil erosion zones of the Songnen Plain in Northeast China. Climate variables played a crucial role in shaping the spatial distribution of SOC stocks at regional scales: they regulated SOC inputs by influencing vegetation types and primary productivity, while also controlling the decomposition and transformation of organic matter through their effects on soil temperature and moisture conditions. Among climatic variables, MAT and MAP exerted particularly significant influences on SOC stocks, with effects that vary markedly across regions. Although prior studies generally highlight a strong correlation between MAP and SOC [31,32], the BRT model results from this study indicated that MAT contributes most substantially to the spatial variability of SOC stocks, with a relative importance of 28% (Figure 5), making it the dominant environmental variable. This finding aligned with multiple previous studies [33,34]. For instance, Mishra et al. [33] identified temperature as a key control on SOC stocks in Northern Hemisphere permafrost regions, while Zhang et al. [32] emphasized in their analysis of spatiotemporal SOC dynamics in high-altitude regions of China that climate—particularly MAT—was the primary variable governing SOC spatial differentiation. Generally, cooler environments were more favorable for SOC accumulation. Collectively, these findings underscore the fundamental regulatory role of climate, especially temperature, in regional SOC stocks and dynamics.

Topographic variables are key variables influencing soil formation and development, as well as the sequestration and dynamics of organic carbon through their regulation of temperature, soil moisture, and evapotranspiration. Terrain governs the decomposition and transformation of SOC by spatially redistributing hydrothermal conditions and regulating vegetation growth, thereby altering litter inputs and the activity levels of soil fauna and microorganisms. Among various terrain attributes, altitude exerts the most pronounced influence (Figure 4), indirectly shaping the accumulation and spatial distribution of organic carbon by modulating temperature and precipitation regimes. For instance, Blackburn et al. [19] reported in a study conducted in North Carolina, USA, that SOC stocks increase significantly with elevation, exhibiting a consistent pattern across different soil depths. SG and SA also substantially influence SOC stocks. Geremew et al. [35] observed that in the Anji River Basin in northwestern Ethiopia-an area characterized by intensive agriculture—SOC content (1.77 Mg ha<sup>-1</sup>) in gently sloping areas (1–15%) was significantly higher than in steep slopes (>30%). TWI is commonly used to represent landscape-scale variations in soil moisture, with higher TWI values generally indicating more favorable moisture conditions that slow down the decomposition and mineralization of organic matter. However, in this study, TWI exhibited the lowest relative importance (RI = 5.8%), which may be attributed to two main factors: first, water flow tends to diverge during its movement from uphill to downhill positions, limiting TWI's ability to accurately reflect actual convergence patterns in lower topographic areas [36]; second, various ecological engineering projects can modify surface topography and underlying surface characteristics, thereby influencing the transport and redistribution of water, sediment, and associated organic matter [37], which may weaken the correlation between TWI and soil organic matter distribution.

# 4.2. Response of SOC Stocks in Different Erosion Zones Under Future Climate Change

As a core component of the black soil region in Northeast China, the Songnen Plain is primarily affected by water erosion in its cultivated areas [38]. In 2023, slight and light

water erosion accounted for 91% of the total eroded area, with corresponding SOC stocks representing approximately 91% of the region's total SOC stocks (Table 3). The prevalence of water erosion in croplands results from the interplay between natural geographical conditions and anthropogenic activities. Although the terrain is predominantly flat, wide-spread gentle slopes (1–3°) facilitate surface runoff due to concentrated summer rainfall—over 70% of annual precipitation occurs between June and September—along with frequent heavy rain events [6]. While black soils naturally possess a favorable granular structure, decades of intensive agricultural practices have led to substantial declines in soil organic matter—locally exceeding 50% loss—and structural degradation, thereby reducing resistance to erosion. Seasonal freeze—thaw cycles further intensify topsoil detachment during spring thaw [7]. Concurrently, agricultural practices such as slope farming, continuous monoculture, and reduced vegetation cover have diminished surface protection and root-mediated soil stabilization. Inadequate drainage infrastructure and underdeveloped protective forest networks have further compromised regional soil and water conservation capacity [22].

However, predictions indicate that by the 2050s, under both the SSP245 and SSP585 climate scenarios, SOC stocks in the region may decrease by 177.66 Tg C and 186.44 Tg C, respectively, with the most pronounced changes occurring in surface soils. As one of the world's key black soil regions, the response mechanism of SOC here is highly complex: increased precipitation can enhance leaching and translocation of organic carbon from the topsoil [39,40]; rising temperatures and altered precipitation patterns jointly accelerate microbial decomposition [41,42]; furthermore, climate change may intensify soil erosion, leading to physical displacement and loss of soil carbon [38]. Consequently, future SOC sequestration in the Songnen Plain will depend not only on improved agricultural management practices but also on addressing the profound impacts of coupled carbon–water cycle dynamics under changing climatic conditions.

In the 2090s, under the SSP245 and SSP585 climate scenarios, SOC stocks in the study area are projected to continue declining, with reductions of 2.84% and 1.41%, respectively. To achieve sustainable socio-economic development, it is imperative to integrate scientific SOC management with adaptive strategies for climate change mitigation. In recent years, China has prioritized black soil conservation by establishing the strategic principle of "protecting black soil as diligently as giant pandas" and implementing a series of supportive policies—such as large-scale straw return programs and the promotion of conservation tillage practices [36,43,44]. The government allocates substantial fiscal resources annually through subsidy mechanisms to incentivize farmers to adopt carbon sequestration-oriented agricultural practices, while also funding multi-billion-yuan research initiatives aimed at enhancing the long-term productivity and sustainability of the black soil region in Northeast China [45]. The findings of this study further validate these efforts. Under the SSP245 and SSP585 scenarios, the implementation of soil conservation such as crop residue return and conservation tillage in the study area is projected to reduce SOC loss to 15.75 Tg C and 7.69 Tg C (Table 3), respectively, by the 2090s, significantly mitigating declines in SOC. Concurrently, rural labor outflows during urbanization have led to partial farmland abandonment, which may facilitate natural SOC accumulation to a certain extent [46]. In the context of global environmental change, accurately projecting the impacts of climate change on regional carbon cycling holds significant scientific value for achieving national "dual carbon" goals, strengthening ecological security, mitigating climate risks, and advancing green, high-quality development. Furthermore, such projections provide a critical theoretical foundation for the formulation of evidence-based ecological policies.

### 4.3. Uncertainties in the Present Study

Based on a high  $R^2$ , LCCC, and low MAE and RMSE, this study selected the BRT model as the optimal model for simulating the spatial distribution of SOC stocks across multiple scenarios. Although the model demonstrates low uncertainty (standard deviation:  $0.41 \pm 0.09$  kg m<sup>-2</sup>), several sources of uncertainty remain in the prediction process.

Firstly, in 2023, soil samples were collected and analyzed by multiple research teams under a unified operational protocol. Nevertheless, systematic uncertainties arising from instrument calibration discrepancies, variations in laboratory conditions, and potential human errors may still affect the accuracy of the modeling data.

Secondly, environmental variable data are derived from multi-platform, multi-resolution remote sensing products and reanalysis datasets, which differ in their original spatial resolution, observation accuracy, and coordinate systems. Although spatial registration and resampling were conducted in ArcGIS 10.2, these preprocessing steps may introduce localized information loss or smoothing effects, potentially compromising the accuracy of the observed relationships between environmental variables and SOC.

Thirdly, although this study included the TWI as a representative microtopographic variable, the omission of other key microtopographic factors—such as profile and planar curvature, flow accumulation, and solar radiation index—may contribute to predictive uncertainty. In flat and eroded landscapes, these variables play a critical role in regulating fine-scale hydrological processes, sediment redistribution, and soil moisture variability, all of which directly affect SOC accumulation and stabilization. Although TWI was incorporated into the model, its low relative importance suggests that either its theoretical basis inadequately captures local soil moisture dynamics or that unmeasured microtopographic interactions exert a stronger influence on SOC distribution in such environments. The lack of a comprehensive microtopographic characterization may therefore result in an underestimation of SOC spatial heterogeneity, particularly in areas where minor surface variations significantly influence carbon storage potential. Future studies should incorporate high-resolution digital elevation models and additional terrain attributes to more accurately represent the multifaceted influence of microtopography on SOC patterns.

Fourthly, the climate data for the historical and future periods are derived from different sources. Specifically, the future climate scenarios are based on downscaled model outputs, which entail greater uncertainty in simulating the frequency and intensity of extreme climate events—such as droughts, rainstorms, and heatwaves—and lack full spatial consistency across climate variables, thereby compromising the reliability of SOC dynamic predictions.

Fifthly, the model training relies on historical soil—environment relationships and does not account for potential significant changes in future soil properties, land use patterns, agricultural management practices, or ecosystem structure. This inherent assumption of static conditions under dynamic realities may amplify prediction errors and constrain the model's capacity for long-term extrapolation.

Sixthly, this study focuses exclusively on SOC stocks in the surface soil layer (0–30 cm) and does not extend to deeper soil layers (e.g., 30–100 cm), which possess greater carbon sequestration potential in the black soil region of the Songnen Plain. Given the considerable depth of the black soil profile and the substantial organic carbon stocks in the subsurface layers, excluding these strata may result in an underestimation of total soil carbon stocks and introduce systematic bias into the assessment of carbon cycling dynamics.

Despite the aforementioned uncertainties, predicting SOC stocks under various future socio-economic development pathways can still provide a critical scientific foundation for black soil conservation and sustainable use. This is particularly important for de-

veloping differentiated farmland management policies, establishing ecological compensation mechanisms, and designing regional carbon neutrality strategies, thereby offering robust decision-making support for soil resource management in the context of climate change.

# 5. Conclusions

This study employed the BRT model and STS method to simulate and predict interannual and decadal dynamics of SOC stocks in the topsoil (0–30 cm) of the Songnen Plain in Northeast China under two climate scenarios (SSP245 and SSP585) for the 2050s and 2090s. The results revealed significant spatial heterogeneity in SOC stocks across the region in 2023. The model identified MAT, elevation, and SA as the three dominant environmental drivers, collectively accounting for approximately 60% of the observed spatial variability. Projections indicated that while the overall source-sink spatial patterns of SOC remained broadly similar under both scenarios, the SSP245 scenario exhibited lower carbon losses and greater carbon sequestration potential, whereas the SSP585 scenario accelerated organic matter decomposition, leading to more pronounced SOC depletion in source areas and reduced accumulation in sink regions. Specifically, compared to the historical baseline period, SOC stocks under the SSP245 and SSP585 scenarios are projected to decrease by 177.66 Tg C and 186.44 Tg C, respectively, by the 2050s. By the 2090s, SOC stocks are expected to decline further by an additional 2.84% and 1.41% under these respective scenarios. Spatially, SOC changes were predominantly concentrated in areas experiencing slight and light water erosion, which accounted for 67% and 22% of total SOC stocks, respectively, underscoring the strong linkage between erosion intensity and carbon cycling processes. These findings provide a scientific basis for regional land managers and policymakers to enhance soil carbon sequestration through optimized agricultural practices and targeted ecological restoration strategies under future climate change, thereby improving the climate resilience and sustainability of black soil ecosystems.

**Author Contributions:** Conceptualization, S.W. and X.Z.; methodology, Q.Z.; software, Z.Y.; validation, Z.W., C.L. and X.Z.; investigation, X.Z.; data curation, X.J.; writing—original draft preparation, S.W.; writing—review and editing, Q.Z.; visualization, Z.Y. All authors have read and agreed to the published version of the manuscript.

**Funding:** This work was funded by the National Key R&D Program of China (Grant No. 2023YFD1501300), National Science Foundation of China (Grant No. 42207289), and Natural Science Foundation of Jilin Province (Grant No. YDZJ202401480ZYTS).

**Data Availability Statement:** The original contributions presented in this study are included in the article. Further inquiries can be directed to the corresponding author(s).

**Acknowledgments:** The authors would like to thank the anonymous reviewers for their valuable comments.

Conflicts of Interest: The authors declare no conflicts of interest.

# References

- Lal, R. Soil carbon sequestration in China through agricultural intensification, and restoration of degraded and desertified ecosystems. Land Degrad. Dev. 2002, 13, 469–478.
- Khan, U. Enriching Soil Organic Carbon for Sustainable Agriculture, Food Security, and Health. J. Indones. Sustain. Dev. Plan. 2024, 5, 67–75.
- 3. Lal, R. Soil carbon sequestration impacts on global climate change and food security. Science 2004, 304, 1623–1627.
- 4. Bouchoms, S.; Wang, Z.; Vanacker, V.; Van Oost, K. Evaluating the effects of soil erosion and productivity decline on soil carbon dynamics using a model-based approach. *Soil* **2019**, *5*, 367–382.

5. Chappell, A.; Webb, N.P.; Leys, J.F.; Waters, C.M.; Orgill, S.; Eyres, M.J. Minimising soil organic carbon erosion by wind is critical for land degradation neutrality. *Environ. Sci. Policy* **2019**, *93*, 43–52.

- 6. He, J.; Gao, C.; Lin, Q.; Zhang, S.; Zhao, W.; Lu, X.; Wang, G. Temporal and spatial changes in black carbon sedimentary processes in wetlands of Songnen Plain, Northeast of China. *PLoS ONE* **2015**, *10*, e0140834.
- 7. Xie, Y.; Tang, J.; Gao, Y.; Gu, Z.; Liu, G.; Ren, X. Spatial distribution of soil erosion and its impacts on soil productivity in Songnen typical black soil region. *Int. Soil Water Conserv. Res.* **2023**, *11*, 649–659.
- 8. Lal, R. Soil erosion and the global carbon budget. Environ. Int. 2003, 29, 437–450.
- 9. Lugato, E.; Paustian, K.; Panagos, P.; Jones, A.; ,Borrelli, P. Quantifying the erosion effect on current carbon budget of European agricultural soils at high spatial resolution. *Glob. Change Biol.* **2016**, *22*, 1976–1984.
- 10. Khan, N.; Jhariya, M.K.; Raj, A.; Banerjee, A.; Meena, R.S. Soil carbon stock and sequestration: Implications for climate change adaptation and mitigation. In *Ecological Intensification of Natural Resources for Sustainable Agriculture*; Springer: Singapore, 2021; pp. 461–489.
- 11. Adhikari, K.; Owens, P.R.; Libohova, Z.; Miller, D.M.; Wills, S.A.; Nemecek, J. Assessing soil organic carbon stock of Wisconsin, USA and its fate under future land use and climate change. *Sci. Total Environ.* **2019**, *667*, 833–845.
- 12. Wang, S.; Xu, L.; Zhuang, Q.; He, N. Investigating the spatio-temporal variability of soil organic carbon stocks in different ecosystems of China. *Sci. Total Environ.* **2021**, *758*, 143644.
- 13. Baldock, J.A.; Wheeler, I.; McKenzie, N.; McBrateny, A. Soils and climate change: Potential impacts on carbon stocks and greenhouse gas emissions, and future research for Australian agriculture. *Crop Pasture Sci.* **2012**, *63*, 269–283.
- 14. Reyes Rojas, L.A.; Adhikari, K.; Ventura, S.J. Projecting soil organic carbon distribution in central Chile under future climate scenarios. *J. Environ. Qual.* **2018**, *47*, 735–745.
- 15. Lal, R.; Kimble, J.; Follett, R.F. Pedospheric processes and the carbon cycle. In *Soil Processes and the Carbon Cycle*; CRC Press: Boca Raton, FL, USA, 2018; pp. 1–8.
- 16. McBratney, A.B.; Santos, M.M.; Minasny, B. On digital soil mapping. Geoderma 2003, 117, 3-52.
- 17. Ma, Y.; Minasny, B.; Malone, B.P.; Mcbratney, A.B. Pedology and digital soil mapping (DSM). Eur. J. Soil Sci. 2019, 70, 216–235.
- 18. Elith, J.; Leathwick, J.R.; Hastie, T. A working guide to boosted regression trees. J. Anim. Ecol. 2008, 77, 802–813.
- 19. Yang, R.; Zhang, G.; Liu, F.; Lu, Y.; Yang, F.; Yang, M.; Zhao, Y.; Li, D. Comparison of boosted regression tree and random forest models for mapping topsoilorganic carbon concentration in an alpine ecosystem. *Ecol. Indic.* **2016**, *60*, 870–878.
- Smith, P.; Davies, C.A.; Ogle, S.; Zanchi, G.; Bellarby, J.; Bird, N.; Braimoh, A.K. Towards an integrated global framework to assess the impacts of land use and management change on soil carbon: Current capability and future vision. *Glob. Change Biol.* 2012, 18, 2089–2101.
- 21. Blackburn, K.W.; Libohova, Z.; Adhikari, K.; Kome, C.; Maness, X.; Silman, M.R. Influence of land use and topographic factors on soil organic carbon stocks and their spatial and vertical distribution. *Remote Sens.* **2022**, *14*, 2846.
- 22. Chen, P.; Xie, Y.; Ren, X.; Cheng, C.; Wei, X. Spatial variation of soil organic carbon density in the black soil region of Northeast China under the influence of erosion and deposition. *J. Clean. Prod.* **2024**, 475, 143616.
- 23. Ren, Y.; Li, X.; Mao, D.; Wang, Z.; Jia, M.; Chen, L. Investigating spatial and vertical patterns of wetland soil organic carbon concentrations in China's Western Songnen plain by comparing different algorithms. *Sustainability* **2020**, *12*, 932.
- 24. Zhao, H.; Luo, C.; Kong, D.; Yu, Y.; Zang, D.; Wang, F. Spatial and Temporal Variations in Soil Organic Matter and Their Influencing Factors in the Songnen and Sanjiang Plains of China (1984–2021). *Land* **2024**, *13*, 1447.
- 25. Liu, H.; Wang, H.; Nong, H.; He, Y.; Chen, Y.; Wang, H.; Yu, M. Opportunities and implementation pathway for China's forestry development under the "Dual Carbon" strategy. *Carbon Res.* **2024**, *3*, 59.
- 26. Zhu, M.; Feng, Q.; Qin, Y.; Cao, J.; Zhang, M.; Liu, W.; Li, B. The role of topography in shaping the spatial patterns of soil organic carbon. *Catena* **2019**, *176*, 296–305.
- 27. Batjes, N.H. Total carbon and nitrogen in the soils of the world. Eur. J. Soil Sci. 1996, 47, 151–163.
- 28. R Development Core Team. R: A Language and Environment for Statistical Computing. R Foundation for Statistical Computing, Vienna, Austria, 2013. Available online: https://www.rproject.org/ (accessed on, 26 July 2025).
- 29. Conrad, O.; Bechtel, B.; Bock, M.; Dietrich, H.; Fischer, E.; Gerlitz, L.; Böhner, J. System for automated geoscientific analyses (SAGA) v. 2.1. 4. *Geosci. Model Dev.* **2015**, *8*, 1991–2007.
- 30. Lin, L. A concordance correlation coefficient to evaluate reproducibility. *Biometrics* **1989**, 45, 255–268.
- 31. Jones, C.; McConnell, C.; Coleman, K.; Cox, P.; Falloon, P.; Jenkinson, D.; Powlson, D. Global climate change and soil carbon stocks; predictions from two contrasting models for the turnover of organic carbon in soil. *Glob. Change Biol.* **2005**, *11*, 154–166.

Agronomy **2025**, 15, 2459 20 of 20

32. Zhang, L.; Zheng, Q.; Liu, Y.; Liu, S.; Yu, D.; Shi, X.; Xing, S.; Chen, H.; Fan, X. Combined effects of temperature and precipitation on soil organic carbon changes in the uplands of eastern China. *Geoderma* **2019**, 337, 1105–1115.

- 33. Mishra, U.; Hugelius, G.; Shelef, E.; Yang, Y.; Strauss, J.; Lupachev, A.; Harden, J.W.; Jastrow, J.D.; Ping, C.L.; Riley, W.J.; et al. Spatial heterogeneity and environmental predictors of permafrost region soil organic carbon stocks. *Sci. Adv.* **2021**, *7*, eaaz5236.
- 34. Huang, Y.; Huang, L.; Qiu, C.; Ciais, P. Evaluation of effects of heat released from SOC decomposition on soil carbon stock and temperature. *Glob. Change Biol.* **2024**, *30*, e17391.
- 35. Geremew, B.; Tadesse, T.; Bedadi, B.; Gollany, H.T.; Tesfaye, K.; Aschalew, A. Impact of land use/cover change and slope gradient on soil organic carbon stock in Anjeni watershed, Northwest Ethiopia. *Environ. Monit. Assess.* **2023**, *195*, 971.
- 36. Fan, W.; Liang, Y.; Yan, J.; Liu, J.; Yuan, J.; Wang, L.; Ren, J.; Cai, H. Creation and application of a full soil layer fertilization technology model for continuous maize cultivation with straw return in black soil of northeast china. *Mosc. Univ. Soil Sci. Bull.* **2024**, 79, 684–692.
- 37. Hu, W.; Shen, Q.; Zhai, X.; Du, S.; Zhang, X. Impact of environmental factors on the spatiotemporal variability of soil organic matter: A case study in a typical small Mollisol watershed of Northeast China. *J. Soils Sediments* **2021**, 21, 736–747.
- 38. Zeng, J.; Fang, H.; Shi, R.; Zhang, H.; Wang, J.; Tan, L.; Guo, Z. Erosion and deposition regulate soil carbon by mediating Fe-Carbon fixation mode in a typical catchment in the black soil region of Northeastern China. *Catena* **2024**, 235, 107704.
- 39. Yu, G.; Fang, H.; Gao, L.; Zhang, W. Soil organic carbon budget and fertility variation of black soils in Northeast China. *Ecol. Res.* **2006**, *21*, 855–867.
- 40. Zhang, G.H.; Yang, Y.; Liu, Y.N.; Wang, Z.Q. Advances and prospects of soil erosion research in the black soil region of Northeast China. *J. Soil Water Conserv.* **2022**, *36*, 1–12.
- 41. Foereid, B.; Lehmann, J.; Major, J. Modeling black carbon degradation and movement in soil. Plant Soil 2011, 345, 223–236.
- 42. Liu, J.; Sui, Y.; Yu, Z.; Shi, Y.; Chu, H.; Jin, J.; Liu, X.; Wang, G. Soil carbon content drives the biogeographical distribution of fungal communities in the black soil zone of northeast China. *Soil Biol. Biochem.* **2015**, *83*, 29–39.
- 43. Guo, H.; Zhao, W.; Pan, C.; Qiu, G.; Xu, S.; Liu, S. Study on the influencing factors of farmers' adoption of conservation tillage technology in black soil region in China: A logistic-ISM model approach. *Int. J. Environ. Res. Public Health* **2022**, *19*, 7762.
- 44. Jiang, M.; Jia, Z.; Wen, Y.; Xu, H.; Wang, H.; Zeng, Y.; Li, L.; Cui, M.; Li, H.; Zhang, J. Safeguarding the "Black Soil Granary": Innovations in Soil Conservation and Sustainable Agriculture. *Bull. Chin. Acad. Sci.* **2024**, *38*, 2024018.
- 45. Zhang, M.; Zhang, H.; Deng, Y.; Yi, C. Effects of Conservation Tillage on Agricultural Green Total Factor Productivity in Black Soil Region: Evidence from Heilongjiang Province, China. *Land* **2024**, *13*, 1212.
- 46. Lu, C.; Luo, X.; Li, H.; Zang, Y.; Ou, Y. Progress and suggestions of conservation tillage in China. *Strateg. Study Chin. Acad. Eng.* **2024**, *26*, 103–112.

**Disclaimer/Publisher's Note:** The statements, opinions and data contained in all publications are solely those of the individual author(s) and contributor(s) and not of MDPI and/or the editor(s). MDPI and/or the editor(s) disclaim responsibility for any injury to people or property resulting from any ideas, methods, instructions or products referred to in the content.